Evidence for proximity of YFe_2Si_2 to a magnetic quantum critical point

David J. Singh*

Department of Physics and Astronomy, University of Missouri, Columbia, Missouri 65211-7010, USA

(Received 20 April 2016; revised manuscript received 8 June 2016; published 29 June 2016)

Calculations of the electronic and magnetic properties of the nonmagnetic metallic compound YFe_2Si_2 are reported. These predict at the density functional level a magnetic state involving ordering along the c axis. This predicted ground state contrasts with experiment, which does not show magnetic order. The electronic structure is three dimensional, and is similar to that of the unconventional superconductor YFe_2Ge_2 as well as that of the high-pressure collapsed tetragonal phase of KFe_2As_2, which is also a superconductor. Based on the results in relation to experiment, we infer that properties of YFe_2Si_2 are strongly influenced by a nearby antiferromagnetic quantum critical point.

DOI: 10.1103/PhysRevB.93.245155

I. INTRODUCTION

There is renewed interest in metals with unusual magnetic behavior. This is due in part to the unusual magnetic properties of the Fe-based superconductors [1–5] and spin-fluctuation pairing models for these and other unconventional superconductors [6–12]. Within such models superconductivity depends both on the details of the spin fluctuations, particularly their strength and momentum dependence, and the electronic structure, i.e., the Fermi surface and the coupling of states on it with the spin fluctuations. In Fe-based superconductors, the electronic structure involves several d orbitals, hybridized with ligand p states, and formed by both hopping through ligand orbitals and direct Fe-Fe hopping. In most cases, this leads to disconnected hole and electron sheets of Fermi surface connected by antiferromagnetic fluctuations associated with a stripe magnetic order [10,11,13]. However, there are heavily electron doped materials, such as $K_xFe_2Se_2$, that apparently only have electron Fermi surfaces, but are still high-temperature superconductors [14–18]. This both presents a challenge for theory and suggests exploration for other compounds that might show different forms of Fe-based superconductivity.

While Fe-based superconductivity has generally been restricted to pnictides and chalcogenides, Zou, Chen, and co-workers [19,20] have recently reported superconductivity in the germanide, YFe_2Ge_2 with $T_c = 1.8$ K. There is strong evidence both from experiment [19,20] and theory [21,22] that the superconductivity is unconventional, but the symmetry of the superconducting state has not been established. In any case, this first finding of Fe-based superconductivity in a compound with a group-IV ligand suggests exploration of chemically related compounds. Here we report investigation of the silicide YFe_2Si_2.

YFe_2Si_2 is an Fe-based compound that occurs in the $ThCr_2Si_2$ structure [23], is metallic, and does not show ordered magnetism in experiment. However, while there is no magnetic ordering, there a significant variation in the reported magnetic properties perhaps due to sample differences [24–32].

Here we present density functional calculations that incorrectly predict a magnetic ground state associated with the Fe atoms. This is in analogy with the recently discovered superconductor YFe_2Ge_2. The details of the magnetic behavior are, however, different suggesting that YFe_2Si_2 may be a very interesting material in relation to the superconductivity and quantum critical behavior in YFe_2Ge_2.

II. METHODS AND STRUCTURE

The present density functional theory (DFT) calculations were done using the generalized gradient approximation of Perdew, Burke, and Ernzerhof (PBE) [33] and the linearized augmented plane-wave (LAPW) method [34] as implemented in the WIEN2K code. [35] LAPW sphere radii of 2.4, 2.4, and 1.85 bohrs were used for Y, Fe, and Si respectively. Well converged basis sets consisting of local orbitals for the upper core states of Y and Fe and LAPW functions up to a cutoff determined by $R_{Si}k_{\max} = 7$, corresponding to an effective $R_{Fe}k_{\max} \simeq 9$ for the metal atoms, were used. The calculations were based on the experimental lattice parameters, $a = 3.92$ Å, $c = 9.92$ Å [23]. The internal coordinate, corresponding to the Si height above the Fe plane, was determined by energy minimization as discussed below.

As mentioned, the internal coordinate of Si in the unit cell was determined by energy minimization. Within our density functional calculations we find a magnetic ground state in contrast to experiment. We did the relaxation both for a non-spin-polarized case and for ferromagnetic order. With ferromagnetic order we obtain a Si position, $z_{\rm Si} = 0.3710$, as compared to 0.3673 without spin polarization. Thus including ferromagnetic order increases the Fe-Si distance from 2.280 to 2.298 Å. To the best of our knowledge there is no reported refinement of the Si position. However, Pinto and Shaked [36] reported a neutron-diffraction study of the related compound, $NdFe_2Si_2$, and obtained a room-temperature Fe-Si bond length of 2.337 Å. This is closer to but still larger than the distance we obtain in the ferromagnetic calculation.

Unless noted otherwise the results presented below are based on the ferromagnetic Si position. Magnetism is predicted in the DFT calculations independent of this choice of Si position. We note that there is a similar but larger effect of magnetism on the structure, particularly the ligand height, in the Fe-based superconductors. This includes compositions that are not magnetically ordered in experiment. In the Fe-based

*singhdj@missouri.edu

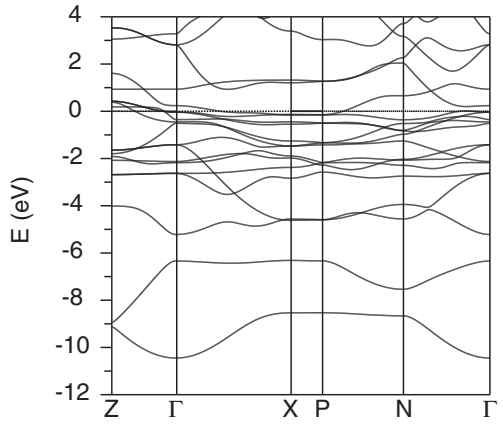

FIG. 1. Calculated non-spin-polarized band structure of YFe_2Si_2.

superconductors the best agreement with the experimental structure is obtained from magnetic calculations [4].

III. RESULTS

We start by discussing the electronic structure as obtained without spin polarization. The calculated band structure is shown in Fig. 1, with the corresponding electronic density of states and projection of Fe d character in Fig. 2. The lowest two bands in Fig. 1 (~ -11 to -6 eV) are from the Si s orbitals, while the higher valence bands shown are derived from Si p and Fe d orbitals. The bands from -3 to 2 eV (relative to the Fermi energy E_F) have predominant Fe character, hybridized with Si. Y occurs as Y^{3+}, with the Y $4d$ states located entirely above E_F as may be expected. The orbital characters of the Fe d bands around E_F are shown in the fat band plots of Fig. 3.

As seen, there are five bands crossing the Fermi level. The resulting five Fermi surfaces are depicted in Fig. 4. These involve multiple d orbitals. The density of states at the Fermi level is $N(E_F) = 5.47$ eV^{-1} per formula unit (two Fe atoms). The corresponding bare specific-heat coefficient is $\gamma_{bare} = 12.9$ mJ/mol K^2. It will be interesting to compare this with

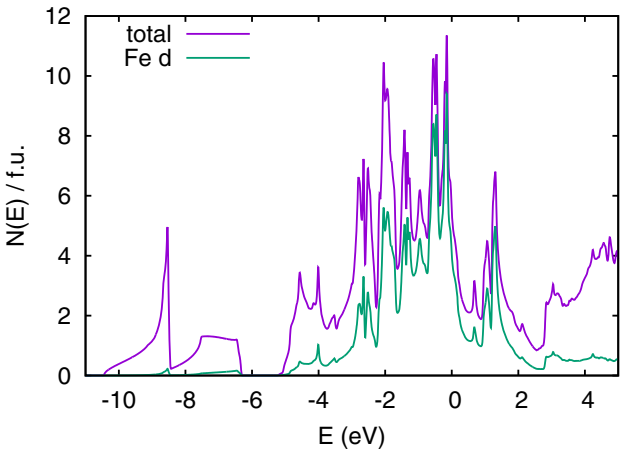

FIG. 2. Calculated electronic density of states and Fe d projection on a per formula unit basis (note that there are two Fe atoms per formula unit).

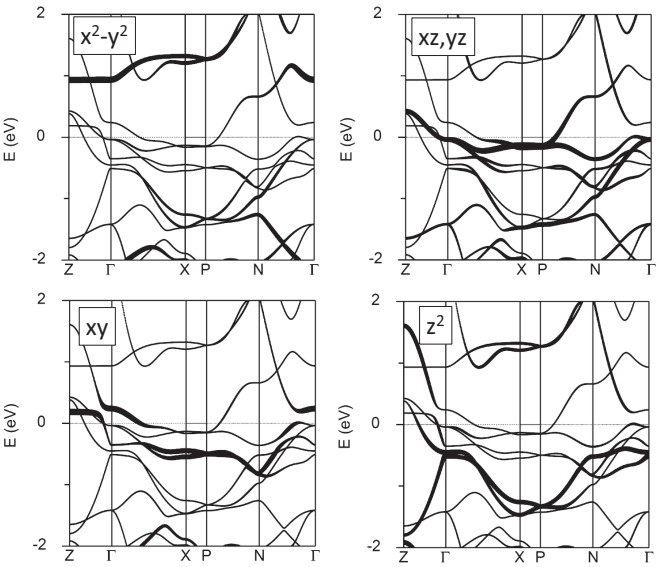

FIG. 3. Bands near the Fermi energy, emphasizing different Fe d orbital characters by fat bands. The coordinate systems for the orbital character is the square lattice defined by the Fe plane, which is rotated 45° from the tetragonal a and b lattice directions for the two Fe atom unit cell.

experiment to determine the specific-heat renormalization, which is $\gamma/\gamma_{bare} \sim 10$ in the germanide superconductor YFe_2Ge_2 [20]. Since $N(E_F)$ comes from d bands, the Stoner criterion for itinerant magnetism [37,38] is clearly exceeded, and so the non-spin-polarized state is unstable against magnetism at the DFT level.

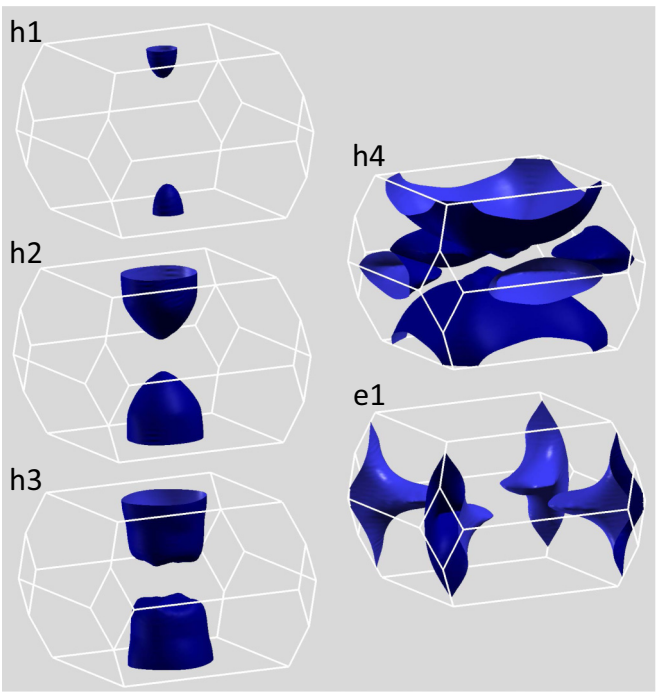

FIG. 4. Fermi surfaces of YFe_2Si_2, showing four hole sheets ($h1$,$h2$,$h3$,$h4$) and one electron sheet ($e1$).

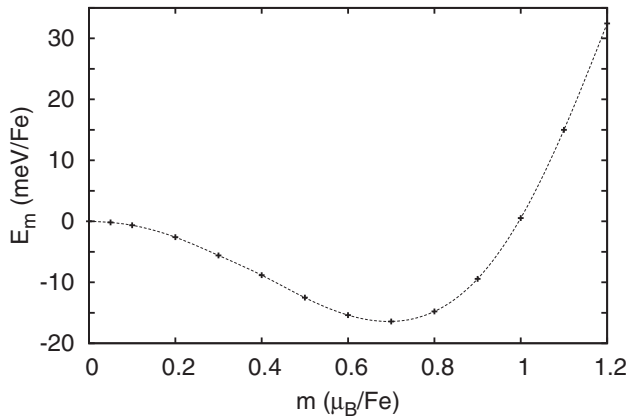

FIG. 5. Fixed spin moment energy as a function of constrained spin magnetization shown on a per Fe atom basis. Note that the values given are from the whole unit cell, and are not the values inside the Fe LAPW sphere.

The calculated plasma frequencies are $\Omega_{p,xx} = \Omega_{p,yy} = 3.33$ eV and $\Omega_{p,zz} = 4.59$ eV. Based on this, YFe_2Si_2 is an anisotropic three-dimensional metal. This means that from an electronic point of view the material is well connected along the c-axis direction. This reflects Si-Si bonding, analogous to the Ge-Ge bonding that has been discussed in YFe_2Ge_2, [20–22] and As-As bonding in the collapsed tetragonal phase of KFe_2As_2 [20]. Assuming that the scattering is relatively k independent, this would imply a high conductivity direction along c, with an anisotropy $\sigma_c/\sigma_a \sim 1.9$. However, as discussed below, the calculations suggest strong spin fluctuations coupled to parts of the Fermi surface, which may produce different scattering on different sheets and a temperature-dependent anisotropy, reflecting the evolution of the spin fluctuations with temperature.

As mentioned, there are five bands crossing E_F. These lead to five sheets of Fermi surface, consisting of four closed hole sections, and an open corrugated cylindrical electron section along the zone corners, as depicted in Fig. 4. The electron count in YFe_2Si_2 is odd, so the electron and hole sections are not compensated, and the hole sections are dominant. The hole sheets consist of four closed sections, $h1$, $h2$, $h3$, and $h4$, centered at the Z point, and containing 0.008, 0.107, 0.154, and 0.893 holes per formula unit, respectively. The electron cylinder at the zone corner ($e1$) contains 0.161 electrons per formula unit. The orbital character of the small $h1$ section is z^2 (here we use the coordinate system of the Fe-square plane, which is rotated 45° with respect to the a and b axes of the two Fe atom unit cell), while the other three hole sections have mixed character involving all the d orbitals except $x^2 - y^2$. The electron cylinder has predominantly xz, yz, and xy character.

As anticipated from the value of $N(E_F)$, which exceeds the Stoner criterion, magnetism is expected at the DFT level. We do find a ferromagnetic instability, as expected. Figure 5 shows the calculated magnetic energy as a function of constrained spin magnetization as obtained from fixed spin moment calculations. As seen, the curvature at zero magnetization is negative, and there is a single ferromagnetic solution. The calculated spin magnetization is $1.39\mu_B$ per two Fe atom unit cell. This comes from a spin moment of $0.75\mu_B$ per Fe (as measured by the magnetization in the Fe LAPW sphere, radius 2.4 bohrs) partly compensated by a back polarization on Si. This is, however, not the calculated ground state.

TABLE I. Calculated energies and total density of states, $N(E_F)$ for different magnetic configurations, on a per formula unit (two Fe) basis, with energies relative to the non-spin-polarized (NSP) state.

	E (eV/f.u.)	$N(E_F)$ (eV^{-1})
NSP	0	5.45
F	−0.033	5.84
C		
G		
A	−0.050	4.08
$A4$	−0.045	4.89
$S1$	−0.026	4.40
$S2$	−0.030	4.29
$S3$	−0.035	4.40
X		
XZ	−0.011	4.87

We did calculations for several different possible orderings, as summarized in Table I. These were ferromagnetic (F), C-type order (C), which is a checkerboard antiferromagnetism in the Fe plane, with like spin Fe stacked on top of each other to make ferromagnetic chains in the c-axis direction, G-type order (G), which is checkerboard in plane stacked antiferromagnetically in the c direction, and A-type order (A), which is ferromagnetic F planes stacked antiferromagnetically. We also did calculations for a double period A type order ($A4$), consisting of double ferromagnetic Fe layers, stacked antiferromagnetically (...UUDDUUDD... along c), stripe type chain order in the Fe planes, as in the Fe-pnictide superconductors, stacked ferromagnetically along c, ($S1$), stacked to run at 90° in alternating planes ($S2$), and stacked antiferromagnetically along c ($S3$). Finally, we consider a double stripe order, which in plane is an X-point order (ferromagnetic Fe chains running diagonally with respect to the Fe square lattice), stacked ferromagnetically along c (X) and antiferromagnetically along c (XZ). Stable solutions were not found for G, C, or X order, and instead imposing these ordering patterns amounted to the non-spin-polarized state.

The results (Table I) show that energy differences between different ordering patterns and the energy difference between the non-spin-polarized state and the ground state are comparable, and some orders do not have solutions at all. This is a signature of itinerant magnetism, in the sense that there are not stable atomic moments that exist independent of the ordering.

It should be noted that magnetic materials are often discussed as either local moment or itinerant, while in fact these are two extreme limiting behaviors that are almost never realized in metallic materials. A useful characterization is that in a material that is close to the local moment limit, the magnetism can be described in terms of interactions between local moments, i.e., the relevant degrees of freedom are the directions of the moments on different sites, as in the Heisenberg or Ising Hamiltonians, while excitations of other spin degrees of freedom are high in energy. In contrast, a material close to the itinerant limit may be characterized

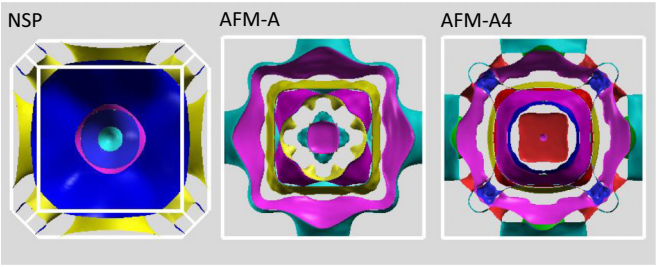

FIG. 6. c-axis view of the Fermi surface for the non-spin-polarized case, and the A-type and $A4$ (see text) orders.

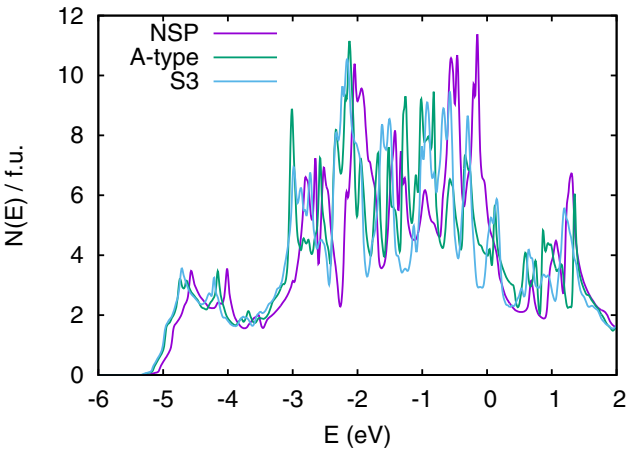

FIG. 7. Density of states for non-spin-polarized, the ground-state A-type antiferromagnetic state, and the $S3$ state.

as having moments that are unstable, in the sense that the moment size depends on the relative orientation. In such cases longitudinal degrees of freedom are important [39] and can be observable. There has been considerable debate around this topic for the Fe-based superconductors, as reviewed, e.g., by Dai [40], based on different experiments, including resonant inelastic x-ray scattering (RIXS) [41]. We also note that there is often a connection drawn between correlated behavior and local moments, although this connection is not strict, as exemplified by the itinerant low-temperature physics of some strongly correlated materials, especially heavy Fermions. In any case, at the DFT level, based on the functional characterization above, the magnetism of YFe_2Si_2 has substantial itinerant character.

The lowest energy orderings are the A type and $A4$ type, with the A-type lower. The lowest energy A-type order also gives the lowest $N(E_F)$, which might suggest a role for electrons at the Fermi energy in stabilizing it. However, examining the other states, there is no clear trend between $N(E_F)$ and energy among the other antiferromagnetic orderings.

The energies show antiferromagnetic stackings along c are favored, but that this is not representable in terms of a single c-axis exchange constant. For example, the energy difference between the A-type and ferromagnetic orders, which differ flipping every c-direction bond from ferromagnetic to antiferromagnetic, is $\sim$27 meV/formula unit, while for the stripe order ($S1$–$S3$) this difference is only 9 meV/formula unit. Finally, and most remarkably, while the $F - A$ energy difference suggests a high energy cost for making ferromagnetic stacking, the $A4$ structure, which has ferromagnetic sheets with half the c-direction bonds ferromagnetic and half antiferromagnetic, has an energy only 5 meV per formula unit above the ground state. The energies therefore suggest an important role for band structure and itinerant electrons in the magnetism.

Returning to the band structure, a twofold degenerate heavy band and a single degenerate band cross E_F at almost the same point along the Γ-Z line. These three bands correspond to the $h2$, $h3$, and $h4$ Fermi surfaces. The crossing is at $\sim$0.19 of the Γ-Z distance. Noting the flattened end of the $h3$ surface and the flattened disk shape of $h4$, there is an implied nesting at a distance of $\sim 0.37 \times 2\pi/c$. This is intermediate between the periodicity of the A and $A4$ magnetic structures (0.5 and 0.25, respectively). Figure 6 shows a view along k_z of the Fermi surfaces for the A and $A4$ magnetic states in comparison with that of the NSP calculation. As seen, these magnetic orders gap away the large parts of these hole sections, in particular producing new reconstructed cylindrical sections from the large hole pancake ($h4$). This suggests that spin fluctuations associated with this order would affect transport in the c-axis direction more strongly than in the plane, leading to a disproportionate reduction in conductivity along c and a temperature-dependent conductivity anisotropy.

This provides an explanation for the stability of these two magnetic structures. It also resolves an experimental puzzle regarding the magnetic structure of the rare-earth substituted compounds. In particular, neutron-diffraction experiments on $NdFe_2Si_2$ found Nd moments ordered with a ferromagnetic in plane order and a c axis . . . UUDDUU . . . order, which was not readily understood in terms of reasonable superexchange pictures [36]. However, Fermi-surface nesting similar to what we find, along with a slight shift in the nesting vector closer to 0.25, could readily explain this pattern.

Figure 7 shows the density of states, comparing the NSP calculations with the lowest energy A-type antiferromagnetic case and the stripe ordered $S3$ case. As seen, the density of states is reconstructed over the energy range of the Fe d bands, i.e., -3 to 2 eV, on going from the NSP state to either of the antiferromagnetic states plotted. This is a characteristic of transition metal magnets and reflects the coupling of the d orbitals. It is the basis of the Stoner theory, which assumes rigid shifts of the d bands on forming ferromagnetic moments [37,38,42,43]. It is a feature of both local moment and itinerant transition metal magnets, and is seen for example in the classic itinerant antiferromagnet Cr [44]. Importantly, comparing the A-type and $S3$ densities of states, it is clear that they similarly differ over the range of the d bands. This is a signature of the importance of band structure effects in the magnetism, including both bands near E_F and bands at energies away from the Fermi level. This is similar to the Fe-based superconductors [45]. It is important to note that the d electrons in any material with magnetism will be subject to exchange coupling. This is the origin of the first Hund's rule. As a consequence, all d electrons will be affected by moment formation regardless of the origin of the magnetism. What is important in assessing the role of different electronic states is then not the shifts upon

moment formation but the energy dependent shifts in spectra between different magnetically ordered configurations.

In the Fe-based superconductors, the role of the electrons near E_F in relation to deeper electronic states has been discussed in connection with the itinerancy of the magnetism. We note that this represents a different use of the term itinerant than above. Spectroscopies clearly show that the magnetism affects the full range of d bands in the Fe-based superconductors and, as discussed above, also couples to core levels, as seen in splitting of the 3s level. In many of the Fe-based superconductors, the stripe antiferromagnetic order couples strongly to the states near E_F and the structure of the Fermi surface is important in selecting the specific stripe order as the ground state. On the other hand, there are competing orders that are not directly related to the Fermi-surface structure leading to a mixed picture [45]. This also appears to be the case in YFe_2Si_2.

Thus, at the DFT level, YFe_2Si_2 is a magnetic compound, with a ground state having ferromagnetic layers, stacked antiferromagnetically, and with a substantial itinerant character. The magnetic order couples strongly to sections of the Fermi surface, particularly the largest hole sheets. The related $A4$ structure is close in energy, and these compete with a strip magnetic order analogous to that of the Fe-based superconductors. In plane checkerboard antiferromagnetism is strongly disfavored. Experimentally, on the other hand no magnetic order is reported. This discrepancy is a key result. We also did PBE + U calculations. As expected, that addition of the Coulomb parameter U further increases the Fe moment opposite to experiment. For an effective $U - J = 5$ eV, with fully localized limit double counting, we obtain a moment of $2.85\mu_B$ in each Fe LAPW sphere for the A-type ordering. This is much higher than the PBE value of $0.76\mu_B$. The discrepancy between DFT calculations and experiment is similar to YFe_2Ge_2 [21,22,46], which is an unconventional superconductor and appears to be near a magnetic quantum critical point (note that $LuFe_2Ge_2$ is magnetically ordered) [19,47].

The experimental situation for YFe_2Si_2 is less clear, perhaps in part because of sample differences. Mössbauer experiments for the isostructural RFe_2Si_2 compounds (R = rare earth) indicated the Fe has no moment in these compounds. However, broadenings were seen in the ^{57}Fe spectra. These were interpreted as originating in induced Fe moments from the rare-earth site [24,25]. Detailed studies show smooth variations in lattice parameters and Mössbauer spectra across the series, similar to the RFe_2Ge_2 compounds [24–26]. The R = La, Y, Lu compounds, where there are no rare-earth moments, are reported to be ordinary Pauli paramagnetic metals [24,27,28]. On the other hand, magnetic behavior is readily inducted by Cr alloying [28], and there are reports that show evidence for multiple Fe sites, with magnetic behavior on a portion of the Fe perhaps associated with Fe-Si disorder [29,30]. Other unusual magnetic behavior has also been reported under pressure and with doping [31,32]. In any case, it is clear that experiment does not show behavior consistent with the A-type magnetic order predicted in DFT calculations.

IV. DISCUSSION AND CONCLUSIONS

The electronic structure of metallic YFe_2Si_2 is found to be very similar to YFe_2Ge_2, including the qualitative structure of the Fermi surface and the band character. Importantly, DFT calculations predict an antiferromagnetic A-type ground state, competing with stripe order. This is in contrast to experiment, which shows Pauli paramagnetism. This type of discrepancy in which standard DFT calculations overestimate the tendency towards magnetism is unusual. More commonly DFT calculations underestimate the tendency towards moment formation as is the case in several classes of strongly correlated materials, including cuprates. Overestimation of the tendency to magnetism in DFT calculations is however a characteristic of the Fe-based superconductors [4]. It is found as well in metals near quantum critical points associated with itinerant magnetism. In that case the discrepancy is a consequence of renormalization by spin fluctuations associated with the critical point and not included in standard DFT calculations [48–50].

The behavior found for YFe_2Si_2 is similar to that found for YFe_2Ge_2, except that (1) the magnetic energy scale is lower in the silicide and (2) the ordering of the magnetic states more strongly favors the A-type ordering relative to ferromagnetism or the stripe orders. It will be of interest to attempt synthesis of high quality well ordered crystals of YFe_2Si_2 in order to measure its physical properties in detail, especially specific heat and transport to assess the extent to which magnetic fluctuations influence its properties. In addition, spectroscopic experiments on Fe-based superconductors and YFe_2Ge_2 have shown evidence of quantum spin fluctuations in splittings of the Fe 3s core level under ambient conditions [5,46]. Similar experiments for YFe_2Si_2 would be of interest.

[1] D. C. Johnston, Adv. Phys. **59**, 803 (2010).
[2] G. R. Stewart, Rev. Mod. Phys. **83**, 1589 (2011).
[3] M. D. Lumsden and A. D. Christianson, J. Phys.: Condens. Matter **22**, 203203 (2010).
[4] I. I. Mazin, M. D. Johannes, L. Boeri, K. Koepernik, and D. J. Singh, Phys. Rev. B **78**, 085104 (2008).
[5] F. Bondino, E. Magnano, M. Malvestuto, F. Parmigiani, M. A. McGuire, A. S. Sefat, B. C. Sales, R. Jin, D. Mandrus, E. W. Plummer, D. J. Singh, and N. Mannella, Phys. Rev. Lett. **101**, 267001 (2008).
[6] D. J. Scalapino, E. Loh, and J. E. Hirsch, Phys. Rev. B **34**, 8190 (1986).
[7] N. D. Mathur, F. M. Grosche, S. R. Julian, I. R. Walker, D. M. Freye, R. K. W. Haselwimmer, and G. G. Lonzarich, Nature (London) **394**, 39 (1998).
[8] M. D. Johannes, I. I. Mazin, D. J. Singh, and D. A. Papaconstantopoulos, Phys. Rev. Lett. **93**, 097005 (2004).
[9] T. Moriya, Proc. Jpn. Acad. B **82**, 1 (2006).
[10] I. I. Mazin, D. J. Singh, M. D. Johannes, and M. H. Du, Phys. Rev. Lett. **101**, 057003 (2008).
[11] K. Kuroki, S. Onari, R. Arita, H. Usui, Y. Tanaka, H. Kontani, and H. Aoki, Phys. Rev. Lett. **101**, 087004 (2008).
[12] D. J. Scalapino, Rev. Mod. Phys. **84**, 1383 (2012).
[13] D. J. Singh and M. H. Du, Phys. Rev. Lett. **100**, 237003 (2008).

[14] J. Guo, S. Jin, G. Wang, S. Wang, K. Zhu, T. Zhou, M. He, and X. Chen, Phys. Rev. B **82**, 180520 (2010).
[15] M. H. Fang, H. D. Wang, C. H. Dong, Z. J. Li, C. M. Feng, and H. Q. Yuan, Europhys. Lett. **94**, 27009 (2011).
[16] L. Zhang and D. J. Singh, Phys. Rev. B **79**, 094528 (2009).
[17] T. Qian, X. P. Wang, W. C. Jin, P. Zhang, P. Richard, G. Xu, X. Dai, Z. Fang, J. G. Guo, X. L. Chen, and H. Ding, Phys. Rev. Lett. **106**, 187001 (2011).
[18] Z. R. Ye, Y. Zhang, F. Chen, M. Xu, J. Jiang, X. H. Niu, C. H. P. Wen, L. Y. Xing, X. C. Wang, C. Q. Jin, B. P. Xie, and D. L. Feng, Phys. Rev. X **4**, 031041 (2014).
[19] Y. Zou, Z. Feng, P. W. Logg, J. Chen, G. Lampronti, and F. M. Grosche, Phys. Status Solidi Rapid Res. Lett. **8**, 928 (2014).
[20] J. Chen, K. Semeniuk, Z. Feng, P. Reiss, P. Brown, Y. Zou, P. W. Logg, G. I. Lampronti, and F. M. Grosche, Phys. Rev. Lett. **116**, 127001 (2016).
[21] A. Subedi, Phys. Rev. B **89**, 024504 (2014).
[22] D. J. Singh, Phys. Rev. B **89**, 024505 (2014).
[23] D. Rossi, R. Marazza, and R. Ferro, J. Less-Common Met. **58**, 203 (1978).
[24] A. M. Umarji, D. R. Noakes, P. J. Viccaro, G. K. Shenoy, A. T. Aldred, and D. Niarchos, J. Magn. Magn. Mater. **36**, 61 (1983).
[25] D. R. Noakes, A. M. Umarji, and G. K. Shenoy, J. Magn. Magn. Mater. **39**, 309 (1983).
[26] J. J. Bara, H. U. Hrynkiewicz, A. Milos, and A. Szytula, J. Less-Common Met. **161**, 185 (1990).
[27] A. Dommann, F. Hulliger, and C. Baerlocher, J. Less-Common Met. **138**, 113 (1988).
[28] I. Ijjaali, G. Venturini, and B. Malaman, J. Alloys Compds. **279**, 102 (1998).
[29] S. G. Sankar, S. K. Malik, V. U. S. Rao, and R. Obermeyer, *Magnetism and Magnetic Materials 1976: Proceedings of the First Joint MMM-Intermag Conference*, AIP Conf. Proc. No. 34, edited by H. C. J. J. Wolfe Becker and G. H. Lander (AIP, New York, 1976), p. 236.
[30] I. Felner, I. Mayer, A. Grill, and M. Schieber, Solid State Commun. **16**, 1005 (1975).
[31] I. Felner, B. Lv, K. Zhao, and C. W. Chu, J. Supercond. Nov. Magn. **28**, 1207 (2015).
[32] I. Felner, B. Lv, and C. W. Chu, J. Phys.: Condens. Matter **26**, 476002 (2014).
[33] J. P. Perdew, K. Burke, and M. Ernzerhof, Phys. Rev. Lett. **77**, 3865 (1996).
[34] D. J. Singh and L. Nordstrom, *Planewaves Pseudopotentials and the LAPW Method*, 2nd ed. (Springer, Berlin, 2006).
[35] P. Blaha, K. Schwarz, G. Madsen, D. Kvasnicka, and J. Luitz, *WIEN2k, An Augmented Plane Wave + Local Orbitals Program for Calculating Crystal Properties* (K. Schwarz, Tech. Univ. Wien, Austria, 2001).
[36] H. Pinto and H. Shaked, Phys. Rev. B **7**, 3261 (1973).
[37] E. C. Stoner, Proc. R. Soc. London Ser. A **169**, 339 (1939).
[38] J. F. Janak, Phys. Rev. B **16**, 255 (1977).
[39] C. Wang, R. Zhang, F. Wang, H. Luo, L. P. Regnault, P. Dai, and Y. Li, Phys. Rev. X **3**, 041036 (2013).
[40] P. C. Dai, Rev. Mod. Phys. **87**, 855 (2015).
[41] C. Wang, Z. C. Wang, Y. M. Mei, Y. K. Li, L. Li, Z. T. Tang, Y. Liu, P. Zhang, H. F. Zhai, Z. A. Xu, and G. H. Cao, J. Am. Chem. Soc. **138**, 2170 (2016).
[42] O. K. Andersen, J. Madsen, U. K. Poulsen, O. Jepsen, and J. Kollar, Physica B **86-88**, 249 (1977).
[43] G. L. Krasko, Phys. Rev. B **36**, 8565 (1987).
[44] H. L. Skriver, J. Phys. F **11**, 97 (1981).
[45] M. D. Johannes and I. I. Mazin, Phys. Rev. B **79**, 220510 (2009).
[46] N. Sirica, F. Bondino, S. Nappini, I. Pis, L. Poudel, A. D. Christianson, D. Mandrus, D. J. Singh, and N. Mannella, Phys. Rev. B **91**, 121102 (2015).
[47] T. Fujiwara, N. Aso, H. Yamamoto, M. Hedo, Y. Saiga, M. Nishi, Y. Uwatoko, and K. Hirota, J. Phys. Soc. Jpn. **76**, 60 (2007).
[48] T. Moriya, *Spin Fluctuations in Itinerant Electron Magnetism* (Springer, Berlin, 1985).
[49] I. I. Mazin and D. J. Singh, Phys. Rev. B **69**, 020402 (2004).
[50] M. Shimizu, Rep. Prog. Phys. **44**, 329 (1981).